Journal of the American College of Cardiology
© 2013 by the American College of Cardiology Foundation
Published by Elsevier Inc.

Vol. 62, No. 19, 2013
ISSN 0735-1097/$36.00
http://dx.doi.org/10.1016/j.jacc.2013.05.076

Protease-Activated Receptor-2 Regulates the Innate Immune Response to Viral Infection in a Coxsackievirus B3–Induced Myocarditis

Alice Weithauser, PhD,*† Peter Bobbert, MD,* Silvio Antoniak, PhD,‡ Andreas Böhm, MSc,§ Bernhard H. Rauch, MD,§ Karin Klingel, MD,‖ Konstantinos Savvatis, MD,* Heyo K. Kroemer, PhD,§ Carsten Tschope, MD,* Andrea Stroux, MSc,¶ Heinz Zeichhardt, PhD,# Wolfgang Poller, MD,* Nigel Mackman, PhD,‡ Heinz-Peter Schultheiss, MD,* Ursula Rauch, MD*

Berlin, Greifswald, and Tübingen, Germany; and Chapel Hill, North Carolina

Objectives This study sought to evaluate the role of protease-activated receptor-2 (PAR2) in coxsackievirus B3 (CVB3)–induced myocarditis.

Background An infection with CVB3 leads to myocarditis. PAR2 modulates the innate immune response. Toll-like receptor-3 (TLR3) is crucial for the innate immune response by inducing the expression of the antiviral cytokine interferon-beta (IFNβ).

Methods To induce myocarditis, wild-type (wt) and PAR2 knockout (ko) mice were infected with 10^5 plaque-forming units CVB3. Mice underwent hemodynamic measurements with a 1.2-F microconductance catheter. Wt and PAR2ko hearts and cardiac cells were analyzed for viral replication and immune response with plaque assay, quantitative polymerase chain reaction, Western blot, and immunohistochemistry.

Results Compared with wt mice, PAR2ko mice and cardiomyocytes exhibited a reduced viral load and developed no myocarditis after infection with CVB3. Hearts and cardiac fibroblasts from PAR2ko mice expressed higher basal levels of IFNβ than wt mice did. Treatment with CVB3 and polyinosinic:polycytidylic acid led to higher IFNβ expression in PAR2ko than in wt fibroblasts and reduced virus replication in PAR2ko fibroblasts was abrogated by neutralizing IFNβ antibody. Overexpression of PAR2 reduced the basal IFNβ expression. Moreover, a direct interaction between PAR2 and Toll-like receptor 3 was observed. PAR2 expression in endomyocardial biopsies of patients with nonischemic cardiomyopathy was positively correlated with myocardial inflammation and negatively with IFNβ expression and left ventricular ejection fraction.

Conclusions PAR2 negatively regulates the innate immune response to CVB3 infection and contributes to myocardial dysfunction. The antagonism of PAR2 is of therapeutic interest to strengthen the antiviral response after an infection with a cardiotropic virus. (J Am Coll Cardiol 2013;62:1737–45) © 2013 by the American College of Cardiology Foundation

An infection with coxsackievirus B3 (CVB3) induces viral myocarditis and dilated cardiomyopathy (1). Viral myocarditis consists of 3 phases: the acute phase with virus entry and replication; the subacute or virus-clearing phase involving innate and adaptive immune responses; and a chronic phase with cardiac remodeling (2). Mice infected with CVB3 exhibit a disease similar to infected patients (3).

A virus infection is initially recognized by Toll-like receptors (TLR). TLRs are pattern-recognition receptors and detect conserved motifs of pathogens. TLR3 recognizes double-stranded ribonucleic acid (dsRNA), an intermediate of viral replication. Activation of TLR3 induces

See page 1746

From the *Department of Cardiology and Pneumology, Charité—Universitätsmedizin Berlin, Berlin, Germany; †Institute for Chemistry-Biochemistry, Freie Universität Berlin, Berlin, Germany; ‡Division of Hematology/Oncology, Department of Medicine, UNC McAllister Heart Institute, University of North Carolina, Chapel Hill, North Carolina; §Department of Pharmacology, Ernst-Moritz-Arndt University, Greifswald, Germany; ‖Department of Molecular Pathology, Institute for Pathology, Eberhard-Karls-University Tübingen, Tübingen, Germany; ¶Department of Biometry and Clinical Epidemiology, Charité–Universitätsmedizin Berlin, Berlin, Germany; and the #Institute of Virology, Charité–Universitätsmedizin Berlin, Berlin, Germany. This study was funded by Deutsche Forschungsgemeinschaft: Sonderforschungsbereich (SFB/TR 19). The authors have reported that they have no relationships relevant to the contents of this paper to disclose.

Manuscript received February 15, 2013; revised manuscript received May 13, 2013, accepted May 13, 2013.

JACC Vol. 62, No. 19, 2013
November 5, 2013:1737–45

Abbreviations and Acronyms

AP = activating peptide
CAR = coxsackievirus-adenovirus receptor
CCL = chemokine ligand
CD = cluster of differentiation
CVB3 = coxsackievirus B3
DAF = decay-accelerating receptor
DMEM = Dulbecco modified Eagle medium
dsRNA = double-stranded ribonucleic acid
FBS = fetal bovine serum
HL = human leukocyte
IFNβ = interferon-beta
IFNγ = interferon gamma
IL = interleukin
ko = knockout
LVEF = left ventricular ejection fraction
mRNA = messenger ribonucleic acid
PAR2 = protease-activated receptor-2
PBS = phosphate-buffered saline
PCR = polymerase chain reaction
p.i. = post-infection
poly(I:C) = polyinosinic: polycytidylic acid
pVitro = mock plasmid
P-Stat1 = phospho-signal transducer and activator of transcription-1
TLR = Toll-like receptor
TNFα = tumor necrosis factor-alpha
wt = wild type

antiviral type 1 interferons, such as interferon-beta (IFNβ) (4). The protease-activated receptor-2 (PAR2) belongs to a family of G-protein–coupled receptors, which are proteolytically activated by serine proteases (5). After infection with herpes simplex virus 1, PAR2 was found to contribute to virus infectivity (6). Similarly, Nhu et al. (7) found that PAR2 suppressed TLR3 signaling and that PAR2 knockout (ko) mice were protected from influenza A virus infections, although another study (8) found different results. In addition, PAR2 was shown to interact with TLR4 and enhance TLR4-dependent signaling (9,10). Therefore, we analyzed if a deficiency of PAR2 influences the development of CVB3-induced myocarditis and heart failure.

Methods

Experimental mouse study. Wild-type (wt) C57Bl/6 mice and PAR2ko mice on a C57Bl/6 background (Martin Steinhoff, Munster, Germany) (11) were housed at the Forschungsinstitut für Experimentelle Medizin (Berlin, Germany). Male mice 6 to 8 weeks old were subdivided into 4 groups. The mice were infected intraperitoneally with 1×10^5 plaque-forming units CVB3 (Nancy Strain) in phosphate-buffered saline (PBS). As control subjects, sham infections with PBS were performed (6 to 8 mice/group) (8 mice/group) for 2, 4, 8, and 28 days. At 28 days post-infection (p.i.) or post-PBS treatment, mice were anesthetized with thiopental (125 μg/kg body weight), artificially ventilated, and hemodynamically characterized with a 1.2-F micro-conductance catheter (12). The experiments were performed in accordance with the National Institutes of Health's Guide for the Care and Use of Laboratory Animals (NIH Pub. No. 85-23, Revised 1996). This study was approved by the Landesamt für Gesundheit und Soziales (Berlin, Germany; no. G100/04).

Clinical pilot study. Between 2009 and 2010, 72 consecutive patients with clinical symptoms of heart failure such as dyspnea (New York Heart Association functional classes II to III) and/or chest pain were included in our pilot study. The presence of ischemic heart disease was excluded in all patients by coronary angiography. All patients underwent an endomyocardial biopsy for histological, immunohistological, and virological examination. The study was approved by the local ethics committee and performed in accordance with the ethics principles in the Declaration of Helsinki. Written informed consent was given by each patient before participation.

Hemodynamic parameters such as left ventricular ejection fraction (LVEF) and left ventricular end-diastolic diameter were determined by angiography and echocardiography. At least 5 endomyocardial biopsies were taken from each patient by using a flexible bioptome (Westmed, Tucson, Arizona) (13). The endomyocardial biopsies were analyzed immunohistologically to assess myocardial inflammation markers such as cluster of differentiation (CD)3+ cells, Mac1, CD45+ cells, human leukocyte (HL) antigen, intercellular adhesion molecule-1, vascular cell adhesion molecule-1, and leukocyte function-associated antigen 1. Cardiac PAR2 and IFNβ expression was determined by quantitative polymerase chain reaction (qPCR). The analysis was performed in blinded fashion by persons unaware of patient data. One of the 72 patients was later found to have amyloidosis and was excluded.

To evaluate the influence of cardiac PAR2 expression, the patients were divided into 2 groups according to their PAR2 expression (lower than the median of PAR2 expression, n = 35; higher than the median, n = 36). Online Table 1 describes the patient characterization.

Cell culture. All cell cultures were maintained in a humidified atmosphere at 37°C and 5% CO_2. The cardiomyocytic HL-1 cell line was kindly provided by Dr. W. C. Claycomb (Louisiana State University Medical Center, Shreveport, Louisiana). HL-1 cardiomyocytes were maintained in precoated culture flasks (0.02% gelatin: 12.5 mg/l fibronectin solution [tebu-bio, Le-Perray-en-Yvelines, France]) in Claycomb medium (JRH Biosciences, Lenexa, Kansas) + 10% fetal bovine serum (FBS) (PAA Laboratories GmbH, Pasching, Germany) + 2 mmol/l l-glutamine (PAA Laboratories GmbH) + 100 U/ml penicillin/streptomycin (PAA Laboratories GmbH) + 0.3 mmol/l ascorbic acid (Sigma-Aldrich, St. Louis, Missouri) and 10 μmol/l norepinephrine (Sigma-Aldrich).

Primary cardiomyocytes and cardiac fibroblasts were isolated from embryonic mouse hearts (embryonic day 13.5) and were maintained in Dulbecco modified Eagle medium (DMEM) without L-glutamine (cardiomyocytes)/DMEM + L-glutamine (fibroblasts) (PAA Laboratories GmbH + 10% FBS + 100 U/ml penicillin/streptomycin. Fibroblasts were used for experiments until the fifth passage (14).

Overexpression of PAR2. Cardiac fibroblasts were transiently transfected with a mock plasmid (pVitro) and a plasmid containing PAR2 (PAR2pVitro) using Lipofectamine 2000 (Invitrogen, Grand Island, New York).

In vitro stimulation. For infection experiments, primary cells were exposed to CVB3 at a multiplicity of infection of

1 in basal DMEM. Thirty minutes after infection, the medium was aspirated and fresh growth medium was added. In replication experiments, a neutralizing anti-mouse-IFNβ (10 μg/ml) (BioLegend, San Diego, California) was added to the medium.

Stimulation with a PAR2 agonist 200 μmol/l 2f-LIGRLO-amide (Calbiochem, San Diego, California), which is designated as an activating peptide (AP), and with a TLR3 agonist polyinosinic:polycytidylic acid (poly[I:C]) (10 μg/ml) (IMGENEX, San Diego, California) was performed in basal DMEM after starvation overnight in DMEM + 0.5% FBS.

Immunohistochemistry. Murine tissue of the left ventricle was embedded in Tissue-Tek (Dako, Glostrup, Denmark). Immunohistochemistry was performed with antibodies against CD3 (1:75; Santa Cruz, Dallas, Texas) and CD68 (1:500; Abcam, Cambridge, Massachusetts). For hematoxylin and eosin staining and in situ hybridization for detection of viral RNA, paraffin-embedded tissue sections were used. The staining procedure and in situ hybridization was performed as previously described (3,15). Images were taken on a Leica microscope (Leica Microsystems, Wetzlar, Germany) and quantifications done with the Lucia software (Lucia Cytogenetics, Prague, Czech Republic).

Plaque assay, Western blot analysis, immunoprecipitation, and real-time PCR. Plaque assay, Western blot, and immunoprecipitation analysis are described elsewhere (15–17). Specific antibodies were used for: phospho-signal transducer and activator of transcription (P-Stat)1 (Abcam); glycerin-aldehyd-3-phosphat-dehydrogenase (Calbiochem), and beta-actin (Santa Cruz); PAR2 (3 μg, clone S-19; Santa Cruz); TLR3 (Abcam); and TLR4 (IMGENEX). For real-time PCR, gene expression was determined with TaqMan PCR using 6-carboxyfluorescein phosphoramidite TaqMan gene expression assays (Applied Biosystems, Invitrogen): tumor necrosis factor (TNF) Mm00443258_m1; interleukin (IL) 1β-Mm00434228_m1; interferon (IFN) γ-Mm00801778_m1; chemokine ligand (CCL) Mm00441243_g1; CCL5 Mm 01302428_m1; IFNβ Mm00446190_m1; IL6 Mm0044 6190_m1; coxsackievirus-adenovirus receptor (CAR) Mm 00438361_m1; decay-accelerating factor (DAF) Mm00438377. Relative gene expression was determined with the comparative C(t) (ΔΔCt) method with 18sRNA Hs99999901_s1 as endogenous control.

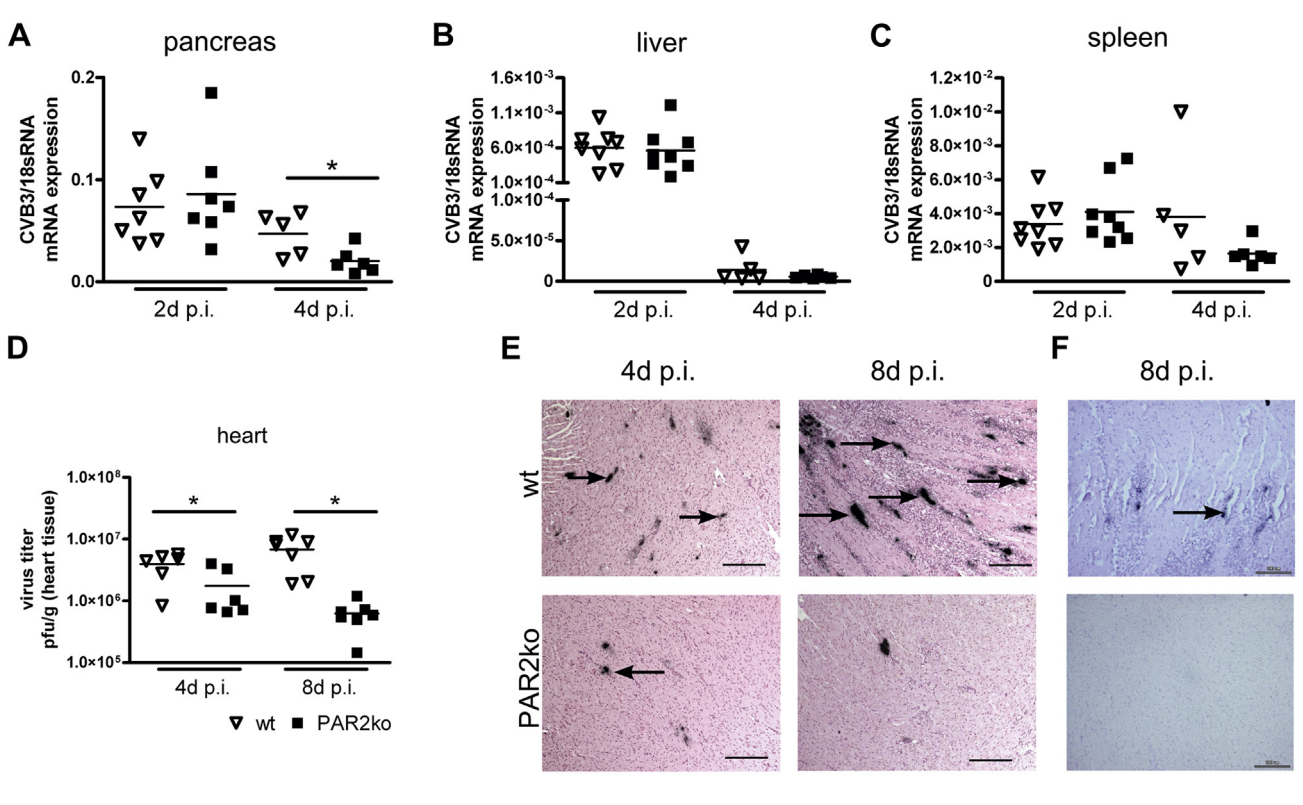

Figure 1 Virus Distribution and Replication in wt and PAR2ko Mice at 2, 4, and 8 Days p.i. With CVB3

(A) The viral genome in pancreas, **(B)** liver, and **(C)** spleen was analyzed with quantitative polymerase chain reaction (qPCR) at 2 and 4 days (d) post-infection (p.i.). **(D)** Plaque assays of wild type (wt) and protease-activated receptor 2 (PAR2) knockout (ko) hearts at 4 and 8 days p.i. Each symbol represents the coxsackievirus B3 (CVB3) messenger ribonucleic acid (mRNA) expression and plaque forming units (pfu) from an individual mouse. **(E)** In situ hybridization of CVB3 plus strand genome of wt and PAR2ko mice at 4 and 8 day p.i. **(F)** In situ hybridization of the minus or replicating strand in hearts at 8 days p.i. **(E, F)** There are 6 to 8 mice for each time point. Scale bar = 100 μm. *$p < 0.05$ for PAR2ko versus respective wt.

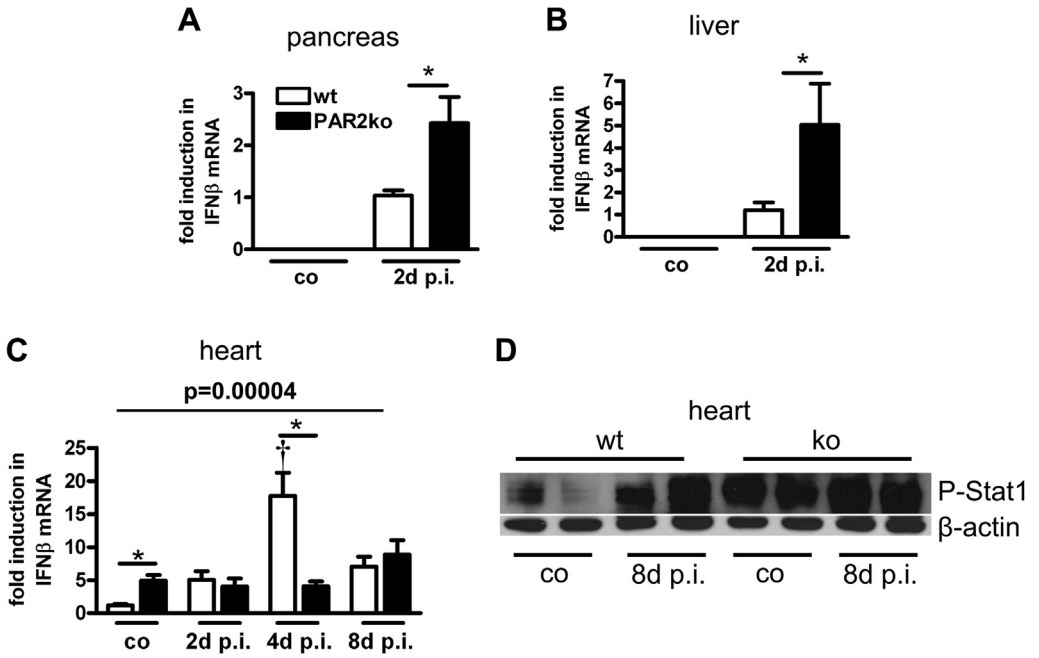

Figure 2 **Up-Regulation of IFNβ Expression and IFNβ-Related Pathways in PAR2ko Mice**

Interferon-beta (IFNβ) expression from infected and control (co) **(A)** pancreas, **(B)** livers, and **(C)** hearts measured by qPCR. **(A, B)** Expression levels are fold to wt at 2 days p.i. (mean was set to 1). **(C)** Expression levels are fold to wt co (mean was set to 1). Data are mean ± SEM (n = 6 to 8 mice/group). *$p < 0.05$ for PAR2ko versus wt, †$p < 0.05$ for PAR2ko versus co mice of the respective genotype and p value according to nonparametric Brunner modeling of longitudinal data. **(D)** Representative Western blot from infected and co hearts shows phospho-signal transducer and activator of transcription-1 (P-Stat1) and beta-actin (β-actin) at 8 days p.i. Abbreviations as in Figure 1.

Statistical analysis. Descriptives include absolute and relative frequencies for categorical variables, and mean ± SD for quantitative variables. Due to lack of normality of most the measurements, the Mann-Whitney *U* test or the Wilcoxon signed rank test have been performed for pairwise comparisons between 2 independent groups or between 2 individual time points, respectively. For longitudinal data analyses, the nonparametric model developed by Brunner et al. (18) has been used, with the genotype as the interindividual factor and the different time points as the intra-individual factor. All statistical analyses have been performed using the commercially available software SPSS (version 21, SPSS Inc., Chicago, Illinois), SAS (version 9.3, SAS Institute, Cary, North Carolina), and/or GraphPad Prism (version 5, San Diego, California). Any p values <0.05 are considered statistically significant. No Bonferroni correction has been applied.

Results

Reduction of virus load in the absence of PAR2. Similar levels of CVB3 were observed in wt and PAR2ko pancreas, liver, and spleen 2 days p.i., whereas the level of CVB3 genomes was significantly lower 4 days p.i. in PAR2ko than in wt pancreas (Fig. 1A). No significant differences in CVB3 genomes were observed in wt and PAR2ko livers and spleens (Figs. 1B and 1C). Plaque assays of a CVB3-infected heart revealed a lower virus load in PAR2ko than in wt hearts at 4 days and 8 days p.i. (Fig. 1D). In situ hybridization showed more positive signals for the plus (genomic) strand of the CVB3 genome in wt than in PAR2ko hearts (Fig. 1E). Sites active of virus replication were evident in wt hearts 8 days p.i. No minus strands were detectable in PAR2ko hearts (Fig. 1F).

CVB3 enters the cell via the CAR (19). CAR messenger ribonucleic acid (mRNA) was significantly increased in wt hearts compared with PAR2ko hearts at 4 days p.i. (Online Fig. 1A). The expression of DAF, a coreceptor for CAR, was also significantly lower in PAR2ko mice than in wt mice at 4 days p.i. (Online Fig. 1B). The baseline expression of CAR and DAF was similar in wt and PAR2ko mice (Online Figs. 1A and 1B).

Increased IFNβ expression in PAR2ko mice. IFNβ is an important early antiviral cytokine that is used to combat CVB3 infection. IFNβ expression was below detection levels in the pancreas and liver of uninfected PAR2ko and wt mice. At 2 days p.i., the pancreas and liver of PAR2ko mice exhibited a higher IFNβ expression than those of wt mice did (Figs. 2A and 2B). Hearts of uninfected PAR2ko had a 5-fold higher IFNβ expression than wt hearts did (Fig. 2C). Reflecting the virus replication, cardiac IFNβ expression was increased in wt mice at 4 days p.i., but not in infected PAR2ko mice (Fig. 2C).

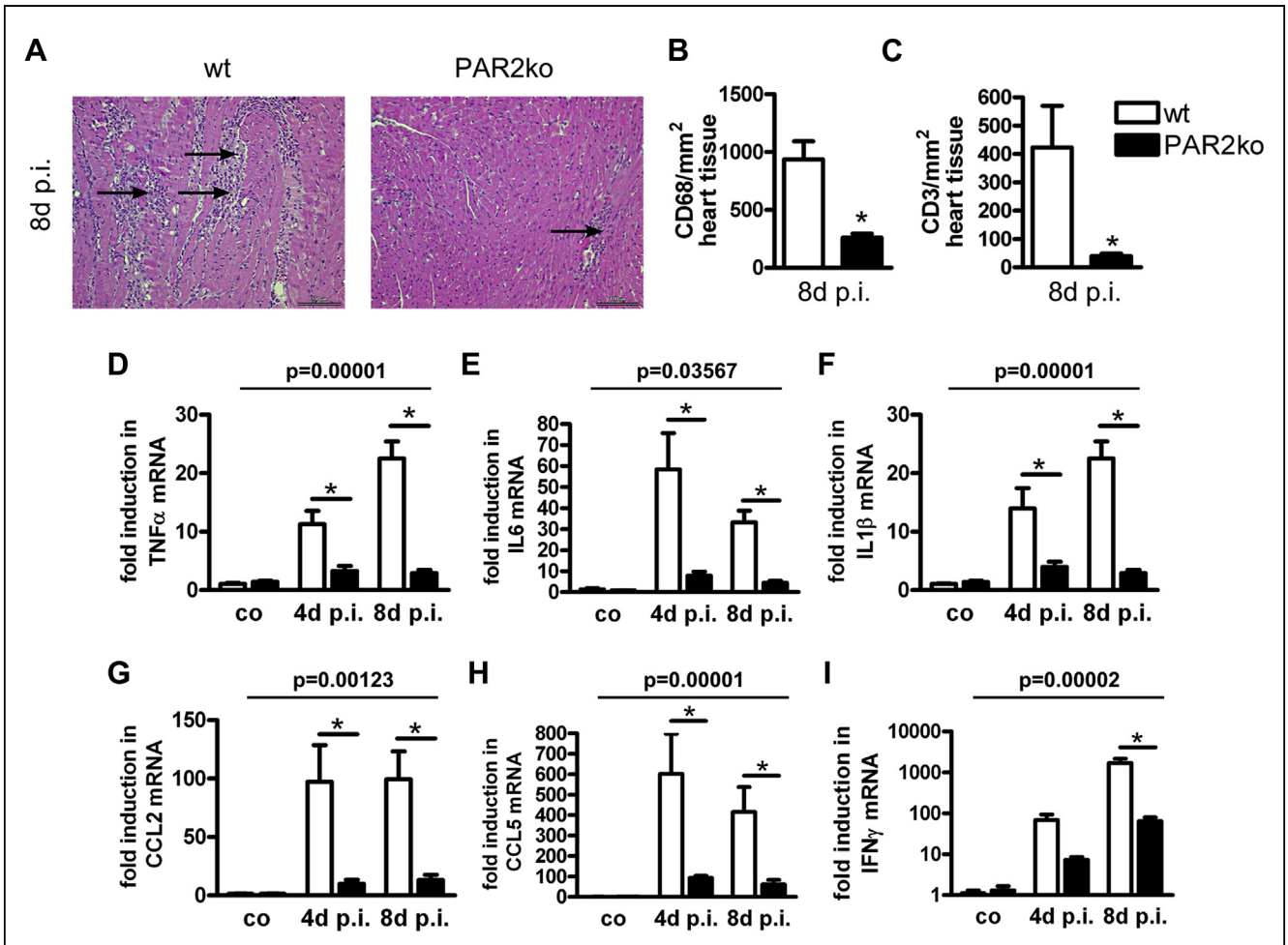

Figure 3 Less Immune Cell Infiltration and Cytokine Expression in PAR2ko Hearts Post-Infection

Hematoxylin and eosin staining of wt and PAR2ko cardiac tissue from co mice and mice at 8 days p.i. **(A) Arrows** indicate immune cell infiltration and tissue damage after CVB3 infection (scale bar = 100 μm). **(B)** Quantification of staining for $CD68^+$ and **(C)** $CD3^+$ cells at 8 days p.i. **(D to I)** Expression of **(D)** TNFα, **(E)** IL6, **(F)** IL1β, **(G)** CCL2, **(H)** CCL5, and **(I)** IFNγ. Expression levels are fold to wt co (mean was set to 1). Data are mean ± SEM (n = 6 to 8 mice/group). *$p < 0.05$ for PAR2ko versus wt and p value according to nonparametric Brunner modeling of longitudinal data. CCL = chemokine ligand; CD = cluster of differentiation; IL = interleukin; TNF = tumor necrosis factor; other abbreviations as in Figures 1 and 2.

IFNβ signaling induces Stat1 phosphorylation. The level of phosphorylated Stat1 was higher in PAR2ko than in wt hearts before infection (Fig. 2D). At 8 days p.i., P-Stat1 was increased in wt and PAR2ko hearts.

PAR2 modulates the immune response. PAR2ko exhibited almost no inflammatory cell infiltration and tissue damage after CVB3 infection (Fig. 3A). Significantly fewer $CD68^+$ and $CD3^+$ cells were seen in PAR2ko than in wt hearts (Figs. 3B and 3C). Additionally, cytokine and chemokine levels were significantly higher in wt than in PAR2ko hearts at 4 and 8 days p.i. (Figs. 3D to 3H). Interferon gamma (IFNγ) mRNA expression was different between the 2 groups at 8 days p.i. but not at 4 days p.i. (Fig. 3I). Over time, both wt and PAR2ko mice showed a significant increase in cytokine expression after infection versus baseline levels, respectively. However, the cytokine expression was always increased to a significantly higher level in wt compared with PAR2ko mice.

PAR2 deficiency protects from CVB3-induced heart failure. A significantly reduced left ventricular function was found in the wt animals at 28 days p.i. compared with left ventricular function at baseline. In contrast, compared with the uninfected mice, the PAR2ko mice exhibited no reduction in heart function at 28 days p.i. The cardiac output was significantly better in PAR2ko than in wt mice at 28 days p.i. (Online Table 2).

Increased IFNβ expression and Stat1 phosphorylation in PAR2ko cardiac fibroblasts. Basal IFNβ expression of primary cardiac fibroblasts was 2.5-fold higher in PAR2ko than in wt fibroblasts. IFNβ expression was also higher in

JACC Vol. 62, No. 19, 2013
November 5, 2013:1737–45

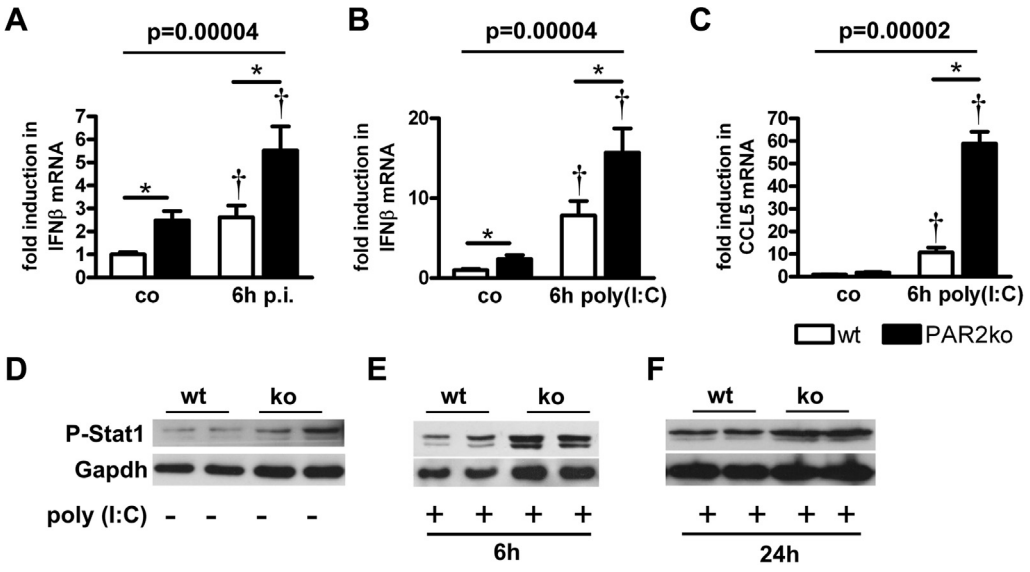

Figure 4 PAR2 Reduces TLR3-Dependent IFNβ and Stat1 Phosphorylation in Cardiac Fibroblasts

(A) IFNβ expression from wt and PAR2ko cardiac fibroblasts infected with 1 multiplicity of infection CVB3 and **(B)** stimulated with 10 μg/ml polyinosinic:polycytidylic acid (poly[I:C]) for 6 h. **(C)** CCL5 expression from wt and PAR2ko cardiac fibroblasts stimulated with 10 μg/ml poly(I:C) for 6 h. Expression levels are fold to wt co (mean was set to 1) (n = 3, performed in duplicates). *$p < 0.05$ for PAR2ko versus wt. †$p < 0.05$ for PAR2ko versus co cells of the respective genotype and p value according to nonparametric Brunner modeling of longitudinal data. **(D to F)** Representative Western blots show phosphorylation for Stat1 in wt and PAR2ko fibroblasts **(D)** before and **(E)** after poly(I:C) stimulation for 6 h and **(F)** 24 h (n = 3). Gapdh = glycerinaldehyd-3-phosphat-dehydrogenase; TLR = Toll-like receptor; other abbreviations as in Figures 1 and 2.

PAR2ko than in wt cells after infection with CVB3 (Fig. 4A). Stimulation with the dsRNA analog poly(I:C) induced IFNβ expression in wt and PAR2ko fibroblasts with significantly higher levels in PAR2ko fibroblasts (Fig. 4B).

Poly(I:C) induced the expression of the IFNβ-regulated gene CCL5 in wt and PAR2ko fibroblasts. As seen for IFNβ, CCL5 mRNA levels were higher in PAR2ko than in wt cells (Fig. 4C). Consistent with our findings in PAR2ko hearts, a higher baseline phosphorylation of Stat1 was observed in PAR2ko fibroblasts compared with wt fibroblasts (Fig. 4D). Stimulation with poly(I:C) for 6 h led to more Stat1 phosphorylation in PAR2ko compared with wt fibroblasts (Fig. 4E). P-Stat levels were also higher at 24 h in stimulated PAR2ko fibroblasts than in wt cells (Fig. 4F).

Virus replication was analyzed 6 and 24 h after infection of PAR2ko and wt cardiomyocytes with CVB3. As seen in mice, compared with wt cardiomyocytes, PAR2ko exhibited a lower virus load 6 and 24 h p.i. Importantly, the virus load in PAR2ko cardiomyocytes increased significantly, and the difference between virus load in the PAR2ko and wt cardiomyocytes was abrogated by a neutralizing IFNβ antibody (Online Fig. 2).

PAR2 activation reduces TLR3-dependent IFNβ expression. To analyze the mechanism by which PAR2 regulates IFNβ expression, PAR2ko primary fibroblasts were transfected with an empty or a PAR2-containing plasmid. PAR2 overexpression in PAR2-deficient fibroblasts reduced the IFNβ expression compared with cells transfected with the empty vector (Fig. 5A). Furthermore, mock- and PAR2-transfected cells were stimulated for 2 and 24 h with poly(I:C) and/or AP, respectively. Stimulation of PAR2 alone did not affect Stat1 phosphorylation in mock- and PAR2-transfected cells, whereas the level of P-Stat1 was strongly increased upon treatment with poly(I:C) in both cell types. Activation with AP and poly(I:C) simultaneously did not affect the P-Stat1 level in mock transfected cells. However, Stat1 phosphorylation was markedly reduced in PAR2 transfected cells treated with the AP and poly(I:C) (Fig. 5B), which is consistent with a PAR2-dependent inhibition of the TLR3 pathway.

Previous studies have shown that PAR2 binds to TLR4 (9). Therefore, we determined if PAR2 physically interacted with TLR3 and TLR4. HL-1 cells were transiently transfected to overexpress PAR2. Cell extracts were immunoprecipitated with an anti-PAR2 antibody and levels of TLR3 within the complex measured by Western blotting. TLR3 and TLR4 were only observed in cells that overexpressed PAR2 and were stimulated with AP (Figs. 5C and 5D).

Myocardial PAR2 expression correlates with the IFNβ expression, myocardial inflammation, and LVEF in patients with cardiomyopathy. Patients with nonischemic cardiomyopathy were divided into 2 groups according to the median cardiac PAR2 expression in the whole study population. IFNβ expression was higher in patients with low PAR2 expressions (Fig. 6A). Patients with a PAR2 mRNA expression above the median had more myocardial infiltrates (Figs. 6B to 6D) and showed a significantly lower LVEF than did patients with a PAR2 expression below the median (Figs. 6E and 6F).

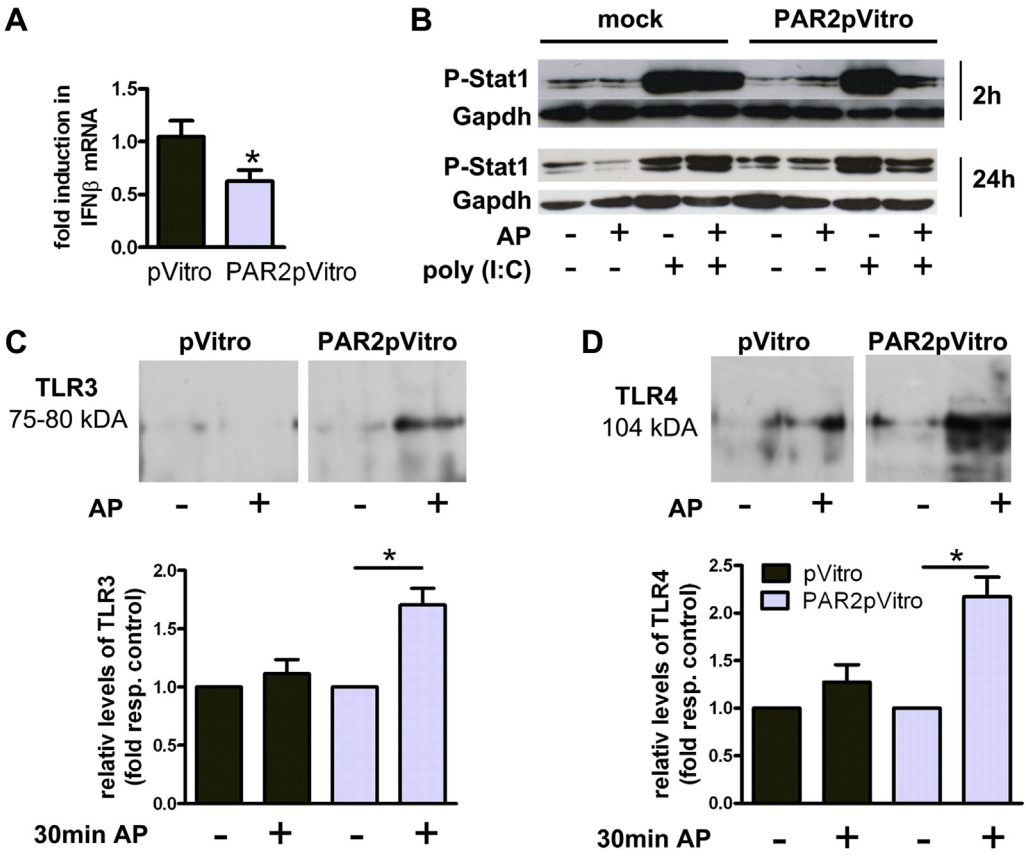

Figure 5 **PAR2 Reduces TLR3-Dependent IFNβ and Stat1 Phosphorylation in Cardiac Fibroblasts**

(A) IFNβ expression in mock plasmid (pVitro)- and PAR2pVitro-transfected PAR2ko fibroblasts. Data are fold to pVitro (mean was set to 1). Data are mean ± SEM (n = 3, performed in duplicates). *p < 0.05 for PAR2ko versus wt. **(B)** Representative Western blots for phosphorylation of Stat1 in pVitro- and PAR2pVitro-transfected PAR2ko fibroblasts before and after stimulation with 200 μmol/l activating peptide (AP) and/or 10 μg/ml poly(I:C) for 2 and 24 h (n = 3). **(C, D)** pVitro- or PAR2pVitro-transfected mouse cardiomyocytic cell line (HL)-1 were stimulated with 200 μmol/l AP for 1 h. Representative Western blots show **(C)** TLR3 and **(D)** TLR4 after PAR2-immunoprecipitation. Densitometry of **(C)** TLR3 and **(D)** TLR4 bands is presented as fold of unstimulated control cells ± SEM. *p < 0.05 (n = 3, performed in duplicates). Abbreviations as in Figures 1, 2, and 4.

Discussion

The study shows that PAR2ko mice are protected from CVB3-induced myocarditis. This was associated with an elevated IFNβ expression in PAR2ko hearts and cardiac fibroblasts. A direct interaction between PAR2 and TLR3 was observed. The PAR2 expression in endomyocardial biopsies of patients with nonischemic cardiomyopathy was positively correlated to myocardial inflammation and negatively with the IFNβ expression and the LVEF.

PAR2 and virus infections. An important finding of this study is that PAR2 contributes to virus infection and severe myocarditis. In line with our data, Nhu et al. (7) observed a higher resistance of PAR2ko mice to influenza-induced pathology than was found with wt mice. In contrast, higher levels of the PAR2 activating enzyme trypsin caused a more severe influenza-induced myocarditis (20).

The CAR expression was increased in hearts of wt mice in contrast to protected PAR2ko mice at 4 days p.i. Similarly, Fuse et al. (21) reported that Myd88ko mice, which were protected from CVB3-induced myocarditis, also exhibited a reduced myocardial CAR expression.

Due to reduced virus levels and inflammation, the left ventricular function was not altered in PAR2ko hearts at 28 days p.i.. In contrast, severe deterioration of myocardial contractility was observed in wt animals. In summary, our in vivo results clearly demonstrate that PAR2 is critical for the development of CVB3-induced myocarditis.

PAR2, the IFNβ pathway, and TLR. A former study demonstrated that IFNβko mice had more severe myocarditis than wt mice did (22). Therapeutic treatment with IFNβ reduced the virus load of CVB3-infected mice (23). In our study, the basal IFNβ levels were significantly increased in PAR2ko hearts and fibroblasts. Furthermore, the overexpression of PAR2 reduced the enhanced basal expression of IFNβ in PAR2ko fibroblasts.

IFNβ signaling induces Stat1 phosphorylation (7), which was basally increased in the absence of PAR2. Given that

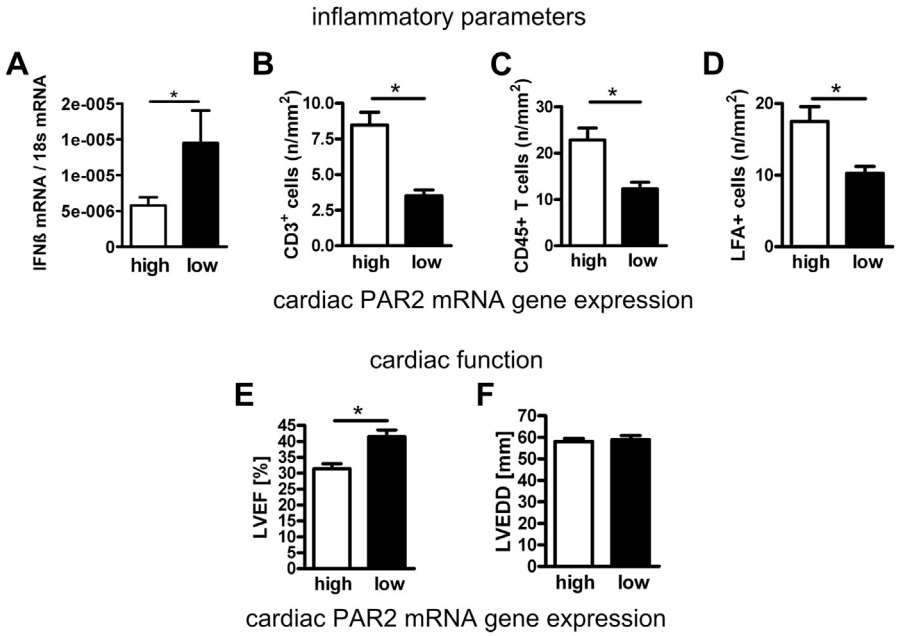

Figure 6 **Cardiac PAR2 Expression in Patients With Cardiomyopathy Is Associated With Increased Cardiac Inflammation, Decreased IFNβ Expression, and Reduced LVEF**

(A) Differences in myocardial IFNβ expression and **(B to D)** CD3+, leukocyte function-associated antigen (LFA)+ and CD45+ cells dependent on low and high myocardial PAR2 expression. **(E, F)** Relations between myocardial PAR2 expression and left ventricular ejection fraction (LVEF) or **(F)** left ventricular end-diastolic diameter (LVEDD). Data are expressed as mean ± SEM. *$p < 0.05$ low versus high PAR2 expression. Abbreviations as in Figures 1 and 3.

neutralizing IFNβ abrogated the diminished virus replication in PAR2ko cardiomyocytes, the basally activated IFNβ pathway is likely to be a reason why less virus replication and inflammation were observed in PAR2ko mice. In summary, PAR2 reduces IFNβ expression and the antiviral immune response.

IFNβ expression is regulated by TLR. In particular by TLR3, which recognizes dsRNA (4). A higher mortality was found in absence of TLR3 upon infection with CVB3 (24). Rallabhandi et al. (9) discovered an AP-dependent physical interaction between PAR2 and TLR4. We found TLR3 co-immunoprecipitated with PAR2 after PAR2 activation with AP. Thus, PAR2 activation can diminish the antiviral response. The physical interaction of PAR2 with TLR3 seems to reduce TLR3-mediated signaling (Online Fig. 3).

PAR2 expression in human heart failure. In a former clinical study with enterovirus- or adenovirus-positive patients, treatment with IFNβ eliminated the virus from the myocardium and improved hemodynamic function (25). PAR2 deficiency also improved the cardiac function in an ischemia/reperfusion injury model (26). To date, a relationship among PAR2 expression, myocardial function, and inflammation in patients is unknown. In a first pilot study on patients with cardiomyopathy, the myocardial PAR2 expression was negatively associated with the myocardial IFNβ expression and the LVEF. In contrast, a positive association was discovered for PAR2 and different inflammatory markers. Whether the PAR2 expression in the heart is predictive for myocardial inflammation and dysfunction in patients with cardiomyopathy remains to be studied.

Conclusions

Cardiac PAR2 is crucial for the genesis of CVB3-induced myocarditis. PAR2 physically interacts with TLR3 and regulates TLR3-dependent IFNβ production in response to an enterovirus infection.

Acknowledgments

The authors would like to thank F. Bleis, K. Kamprath, and M. Pippow for excellent technical support.

Reprint requests and correspondence: Dr. Ursula Rauch, Charité–Universitätsmedizin Berlin, Campus Benjamin Franklin, Department of Cardiology and Pneumology, Hindenburgdamm 30, 12200 Berlin, Germany. E-mail: ursula.rauch@charite.de.

REFERENCES

1. Liu PP, Yan AT. Cardiovascular magnetic resonance for the diagnosis of acute myocarditis: prospects for detecting myocardial inflammation. J Am Coll Cardiol 2005;45:1823–5.

2. Esfandiarei M, McManus BM. Molecular biology and pathogenesis of viral myocarditis. Annu Rev Pathol 2008;3:127–55.
3. Klingel K, Hohenadl C, Canu A, et al. Ongoing enterovirus-induced myocarditis is associated with persistent heart muscle infection: quantitative analysis of virus replication, tissue damage, and inflammation. Proc Natl Acad Sci USA 1992;89:314–8.
4. Alexopoulou L, Holt AC, Medzhitov R, Flavell RA. Recognition of double-stranded RNA and activation of NF-kappaB by Toll-like receptor 3. Nature 2001;413:732–8.
5. Coughlin SR. Thrombin signalling and protease-activated receptors. Nature 2000;407:258–64.
6. Sutherland MR, Ruf W, Pryzdial EL. Tissue factor and glycoprotein C on herpes simplex virus type 1 are protease-activated receptor 2 cofactors that enhance infection. Blood 2012;119:3638–45.
7. Nhu QM, Shirey K, Teijaro JR, et al. Novel signaling interactions between proteinase-activated receptor 2 and Toll-like receptors in vitro and in vivo. Mucosal Immunol 2010;3:29–39.
8. Khoufache K, LeBouder F, Morello E, et al. Protective role for protease-activated receptor-2 against influenza virus pathogenesis via an IFN-gamma-dependent pathway. J Immunol 2009;182:7795–802.
9. Rallabhandi P, Nhu QM, Toshchakov VY, et al. Analysis of proteinase-activated receptor 2 and TLR4 signal transduction: a novel paradigm for receptor cooperativity. J Biol Chem 2008;283:24314–25.
10. Williams JC, Lee RD, Doerschuk CM, Mackman N. Effect of PAR-2 deficiency in mice on KC expression after intratracheal LPS administration. J Signal Transduct 2011;2011:415195.
11. Damiano BP, Cheung WM, Santulli RJ, et al. Cardiovascular responses mediated by protease-activated receptor-2 (PAR-2) and thrombin receptor (PAR-1) are distinguished in mice deficient in PAR-2 or PAR-1. J Pharmacol Exp Ther 1999;288:671–8.
12. Antoniak S, Boltzen U, Riad A, et al. Viral myocarditis and coagulopathy: increased tissue factor expression and plasma thrombogenicity. J Mol Cell Cardiol 2008;45:118–26.
13. Kühl U, Pauschinger M, Seeberg B, et al. Viral persistence in the myocardium is associated with progressive cardiac dysfunction. Circulation 2005;112:1965–70.
14. Boltzen U, Eisenreich A, Antoniak S, et al. Alternatively spliced tissue factor and full-length tissue factor protect cardiomyocytes against TNF-alpha-induced apoptosis. J Mol Cell Cardiol 2012;52:1056–65.
15. Szotowski B, Goldin-Lang P, Antoniak S, et al. Alterations in myocardial tissue factor expression and cellular localization in dilated cardiomyopathy. J Am Coll Cardiol 2005;45:1081–9.
16. Rauch BH, Millette E, Kenagy RD, Daum G, Clowes AW. Thrombin- and factor Xa-induced DNA synthesis is mediated by transactivation of fibroblast growth factor receptor-1 in human vascular smooth muscle cells. Circ Res 2004;94:340–5.
17. Fechner H, Pinkert S, Wang X, et al. Coxsackievirus B3 and adenovirus infections of cardiac cells are efficiently inhibited by vector-mediated RNA interference targeting their common receptor. Gene Ther 2007;14:960–71.
18. Brunner E, Domhof S, Langer F. Nonparametric Analysis of Longitudinal Data in Factorial Experiments. New York, NY: Wiley, 2002.
19. Shi Y, Chen C, Lisewski U, et al. Cardiac deletion of the Coxsackievirus-adenovirus receptor abolishes coxsackievirus B3 infection and prevents myocarditis in vivo. J Am Coll Cardiol 2009;53:1219–26.
20. Pan HY, Yamada H, Chida J, et al. Up-regulation of ectopic trypsins in the myocardium by influenza A virus infection triggers acute myocarditis. Cardiovasc Res 2011;89:595–603.
21. Fuse K, Chan G, Liu Y, et al. Myeloid differentiation factor-88 plays a crucial role in the pathogenesis of coxsackievirus B3-induced myocarditis and influences type I interferon production. Circulation 2005;112:2276–85.
22. Deonarain R, Cerullo D, Fuse K, Liu PP, Fish EN. Protective role for interferon-beta in coxsackievirus B3 infection. Circulation 2004;110:3540–3.
23. Wang YX, da Cunha V, Vincelette J, et al. Antiviral and myocyte protective effects of murine interferon-beta and -{alpha}2 in coxsackievirus B3-induced myocarditis and epicarditis in Balb/c mice. Am J Physiol Heart Circ Physiol 2007;293:H69–76.
24. Negishi H, Osawa T, Ogami K, et al. A critical link between Toll-like receptor 3 and type II interferon signaling pathways in antiviral innate immunity. Proc Natl Acad Sci U S A 2008;105:20446–51.
25. Kühl U, Pauschinger M, Schwimmbeck PL, et al. Interferon-beta treatment eliminates cardiotropic viruses and improves left ventricular function in patients with myocardial persistence of viral genomes and left ventricular dysfunction. Circulation 2003;107:2793–8.
26. Antoniak S, Rojas M, Spring D, et al. Protease-activated receptor 2 deficiency reduces cardiac ischemia/reperfusion injury. Arterioscler Thromb Vasc Biol 2010;30:2136–42.

Key Words: interferon beta ▪ myocarditis ▪ protease-activated receptor 2 ▪ Toll-like receptor 3.

APPENDIX

For supplemental tables and figures, please see the online version of this article.